American Journal of Nanosciences
2016; 2(4): 46-50
http://www.sciencepublishinggroup.com/j/ajn
doi: 10.11648/j.ajn.20160204.12

Studying Structural and Optical Properties of Thin Films $LiNi_xMn_{2-x}O_4$ (x = 0, 0.4, 0.5, 0.6) Prepared by Sol-Gel Method

Adnan Hafez Mini[1], Mohammad Bashir Karaman[2], Ahmed Khaled Kbetri[1, *]

[1]Department of Physics, College of Science, Tishreen University, Latakia, Syria

[2]Department of Physics, College of Science, Aleppo University, Aleppo, Syria

Email address:

ahmed.kbetri@gmail.com (A. K. Kbetri)

[*]Corresponding author

To cite this article:

Adnan Hafez Mini, Mohammad Bashir Karaman, Ahmed Khaled Kbetri. Studying Structural and Optical Properties of Thin Films $LiNi_xMn_{2-x}O_4$ (x = 0, 0.4, 0.5, 0.6) Prepared by Sol-Gel Method. *American Journal of Nanosciences.* Vol. 2, No. 4, 2016, pp. 46-50.
doi: 10.11648/j.ajn.20160204.12

Received: October 14, 2016; **Accepted:** November 18, 2016; **Published:** December 12, 2016

Abstract: Thin films $LiNi_xMn_{2-x}O_4$ (x=0, 0.4, 0.5, 0.6) were prepared by Sol-Gel method employing spin-coated technique. The films were annealed at 600°C for 2 hours. The structural properties of the films were studied by XRD technique. The films were found in cubic spinel structure with decreasing in the lattice constant by increasing the substitution ratio until x=0.5. After this ratio additional peaks appearing in XRD pattern, this indicates a phase transition of $LiNi_{0.6}Mn_{1.4}O_4$ thin film. Optical properties of the $LiNi_xMn_{2-x}O_4$ thin films were investigated by UV–VIS spectroscopy in [400-900] nm rang. The study indicated the presence of a high absorbency values in some part of visible range spectrum of the $LiNi_xMn_{2-x}O_4$ thin films. Direct optical band gap for thin films $LiNi_xMn_{2-x}O_4$ were estimated.

Keywords: Thin Films, $LiNi_xMn_{2-x}O_4$, Sol-Gel, XRD Properties, Optical Properties

1. Introduction

In recent years, electronic devices have been considerably improved in integration and power consumption but improvements in size of the power source have been relatively slow compared with others. Therefore, establishing thin-film technologies for lithium ion batteries is an important step towards all-solid-state thin films batteries that are attractive for portable devices [1-3]. Thin films battery consist of three fundamental components: two electrodes referred to as cathode and anode, and an electrolyte [4]. There are efforts in the development of improved electrolyte and anode materials, but the focus of this paper is on the cathode materials.

Cathode materials are typically oxides of transition metals, and one of the most promising cathode materials for rechargeable lithium batteries is spinel $LiMn_2O_4$, due to low toxicity, low cost and much safer in comparing with layered structure, like $LiCoO_2$ and $LiNiO_2$ [5].

Thin-film electrodes are often prepared by physical vapor deposition methods such as pulsed laser deposition [6], sputtering deposition [7, 8]. These methods ensure control over uniformity and thickness of the films, but are limited with respect to substrate sizes and pricing. Wet chemical Sole-Gel techniques are low cost, flexible with regard to substrate size and geometry [9], and can overcome the disadvantages of physical vapor deposition methods growth, such as slow deposition rate.

$LiMn_2O_4$ exhibits a normal spinel structure with the Li^+ ions occupying the tetrahedral sites and a 1:1 mixture of Mn^{3+} and Mn^{4+} ions being randomly distributed over the octahedral sites [10, 11]. Fig. 1 is shown crystal structure of spinel $LiMn_2O_4$ [12].

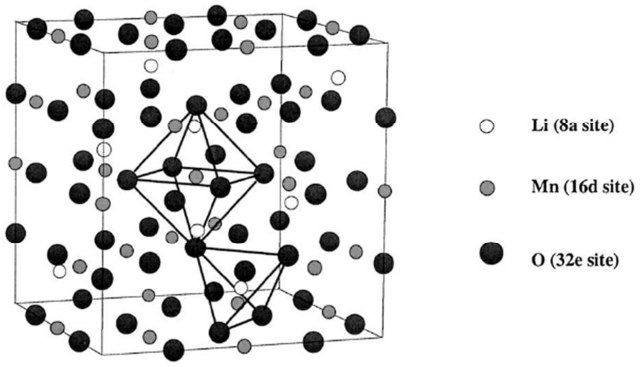

Fig. 1. *Crystal structure of spinel $LiMn_2O_4$.*

The existence of Mn^{3+} ions in the octahedral sites of $LiMn_2O_4$ tends to induce a Jahn-Teller (JT) effect that is likely to cause structural instability during charge discharge cycling [13]. An efficient way to improve this spinel is to substitute Mn by transition metal (M) such as Ti, Co, Mg, Ni and Al [14]. In the present study, thin films $LiNi_xMn_{2-x}O_4$ (x= 0, 0.4, 0.5, 0.6) were synthesized using a Sol-Gel method. The effects of Ni substitution on the structural and the optical properties were investigated by using X-ray diffraction (XRD) and UV–VIS spectroscopy technique.

2. Experimental

$LiNi_xMn_{2-x}O_4$ thin films were deposited on sodalime glass substrates using a sol–gel method. For $LiNi_xMn_{2-x}O_4$ thin films, the precursors solutions was prepared by dissolving LiCl, $(CH_3COO)_2.Mn.4H_2O$ and $Ni(NO_3)_2.6.H_2O$ powders together in ethanol with adding dimethylamine. All chemicals that used were supplied by Sigma – Aldrich. The molar ratio Li:Ni:Mn in the precursor solution was as it shown in table 1.

Table 1. *The molar ratio Li:Ni:Mn in the precursor solution.*

x	0	0.4	0.5	0.6
Li:Ni:Mn	1:0:2	1:0.4:1.6	1:0.5:1.5	1:0.6:1.4

The substrate was spin-coated by the precursor solution at 4000 rpm for 30 s and then heated at 170°C for 2 min followed by 300°C for 5 min after each deposition in order to remove the organic substance. This process was repeated until the desired film thickness was attained. Then the precursor films were annealed in air at 600°C for 2 h. Prior to the film deposition, the substrates were cleaned by alkali solution method. The thickness of the obtained films by the above process was about 100 nm, determined by spectra manager software program linked with spectroscopy device JASCO v650.

The crystalline structure of the samples was monitored by XRD using Cu Kα radiation, using Leybold X-RAY Apparatus device (λ = 1.5405 Å), The diffraction data were recorded for 2θ between 10° and 70°. The optical properties of the films were investigated by using JASCO v650 spectroscopy device in range [400-900] nm.

3. Results and Discussion

3.1. Structural Properties

The XRD patterns of the $LiNi_xMn_{2-x}O_4$ (x = 0, 0.4, 0.5, 0.6) samples are displayed in Fig. 2. These patterns were compared with the JCPDS (JCPDS 35-0782) pattern of $LiMn_2O_4$ [15], and that indicates that crystal structure of thin films was formed according to a cubic spinel structure except for thin film $LiNi_{0.6}Mn_{1.4}O_4$. For ratio x=0.6 additional peaks appearing at the right side of the (311) diffraction peak, and on the left side of the (400) diffraction peak as marked by * in Fig. 2, this indicates a phase transition for this ratio and the structure of this ratio is no longer a cubic spinel structure. The diffraction lines shifted towards higher 2θ angles with Ni substitution, indicating that the lattice parameter decreased with Ni content increase. The lattice constant a_0 for thin films $LiNi_xMn_{2-x}O_4$ with cubic spinel structure (x=0, 0.4, 0.5) were calculated using equations (1) [16].

$$d = \frac{a_0}{\sqrt{h^2 + k^2 + \ell^2}} \quad (1)$$

Where h k ℓ is miller index, d distance between parallel planes.

The distance between parallel planes is calculated using Bragg's law of X-ray diffraction using equation (2) [16].

$$n \cdot \lambda = 2 \cdot d \cdot \sin\theta \quad (2)$$

Where n is a positive integer and λ is the wavelength of incident wave.

The value of distance between parallel planes, lattice constant and volume of primary cell for thin films $LiNi_xMn_{2-x}O_4$ with (x=0, 0.4, 0.5) are listed in table 2.

Table 2. *Structural parameters of the thin films $LiNi_xMn_{2-x}O_4$ with (x= 0, 0.4, 0.5).*

Sample	Distance of parallel plans d Å	Lattice constant a_0 Å	volume of primary cell VÅ^3
$LiMn_2O_4$	2.056	8.224	556.223
$LiNi_{0.4}Mn_{1.6}O_4$	2.047	8.188	548.950
$LiNi_{0.5}Mn_{1.5}O_4$	2.043	8.172	545.739

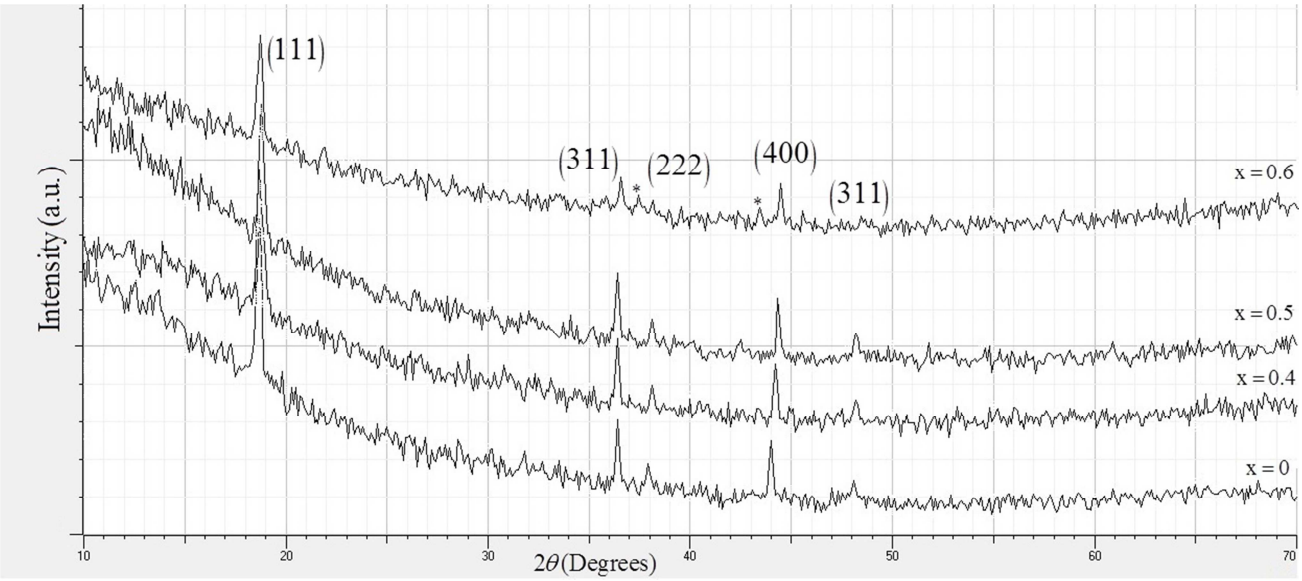

Fig. 2. *XRD spectra of $LiNi_xMn_{2-x}O_4$ thin films fabricated on glasses substrates.*

These values are compatible with previous studies where a_0 for thin film $LiMn_2O_4$ is 8.225 Å in reference [17], for thin film $LiNi_{0.4}Mn_{1.6}O_4$ is 8.174 Å in reference [18], and for thin film $LiNi_{0.5}Mn_{1.5}O_4$ is 8.170 Å in reference [19]. To indicate the impact of the substitutions ratio x on the lattice constant we draw variation of the lattice parameters as a function of Ni content x in spinel $LiNi_xMn_{2-x}O_4$ as shown in Fig. 3.

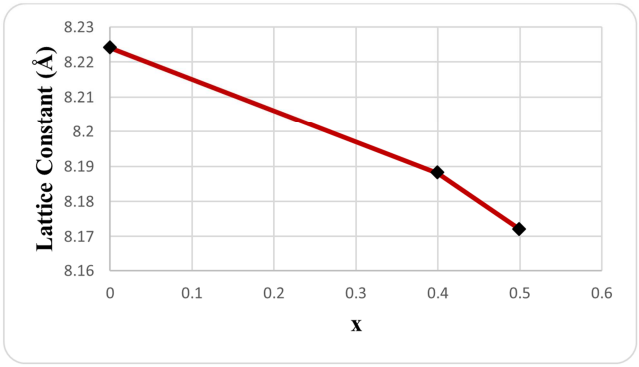

Fig. 3. *Variation of the lattice parameters as a function of Ni content x in spinel $LiNi_xMn_{2-x}O_4$.*

The decrease of the lattice parameters with Ni substitution in $LiNi_xMn_{2-x}O_4$ can be explained depending on bond length between Mn(Ni) and O in the compound $LiNi_xMn_{2-x}O_4$. The Mn(Ni)-O bond increased slightly with Ni substitution because of the larger atomic weight of Ni than Mn. The length bond Mn-O in compound $LiMn_2O_4$ is 1.823 Å [20], the length bond Mn(Ni)-O in compound $LiNi_{0.4}Mn_{1.6}O_4$ is 1.804 Å and in compound $LiNi_{0.5}Mn_{1.5}O_4$ is 1.800 Å [18]. So a decreases in volume of primary cell happened.

3.2. Optical Properties

UV–VIS spectroscopy is a very useful technique for estimating the optical band gap of a semiconductor. The optical band gap is very much related to the electronic conductivity of the materials. Fig. 4 shows the UV–VIS absorption spectra of thin films $LiNi_xMn_{2-x}O_4$. The spectra are plots of absorbance against wavelength of the photon at normal incidence and at room temperature for the thin films. The UV-VIS spectra shows that the films have high absorbance in some parts of the visible region, which decreases gradually as the wavelength increases.

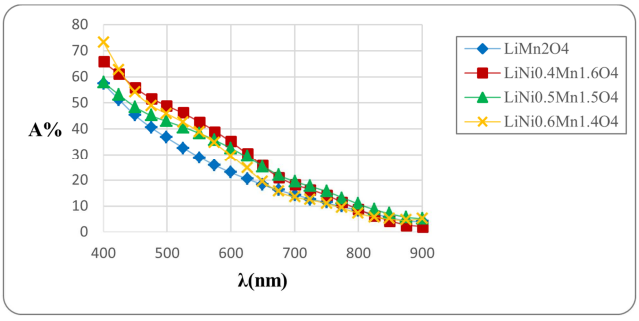

Fig. 4. *Absorbance against wavelength for $LiNi_xMn_{2-x}O_4$ (x=0, 0.4, 0.5, 0.6) thin films.*

Band gap of the thin films where calculated for direct allowed transition by equation (3) [17]:

$$\alpha \cdot h\upsilon = A_1 \left(h\upsilon - E_g \right)^{1/2} \quad (3)$$

Where, A_1 is a constant related to characteristics of valence packs and conductivity packs of the semiconductor, E_g the energy band gap, hν energy of the photon, α absorption coefficient.

By presenting $(\alpha h\nu)^2$ values as a function to hν Graphically, and extension of the linear part of the curve graph to crossing the hν axis, then the energy gap will be determined as it is shown in Fig. 5, Fig. 6, Fig. 7, and Fig. 8 for thin films $LiMn_2O_4$, $LiNi_{0.4}Mn_{1.6}O_4$, $LiNi_{0.5}Mn_{1.5}O_4$, and $LiNi_{0.6}Mn_{1.4}O_4$ respectively. The direct band gap for thin films were estimated and listed in table 3.

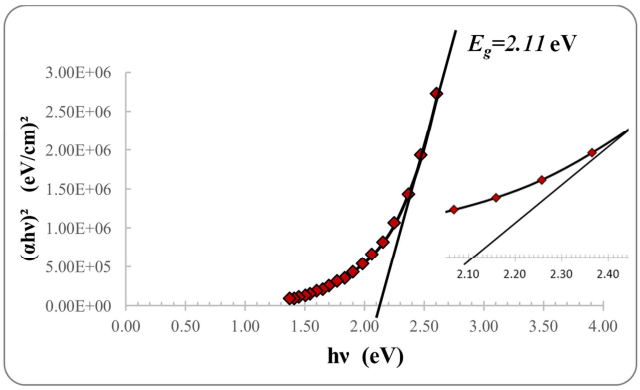

Fig. 5. *$(\alpha h\nu)^2$ values as a function to hν for thin film $LiMn_2O_4$.*

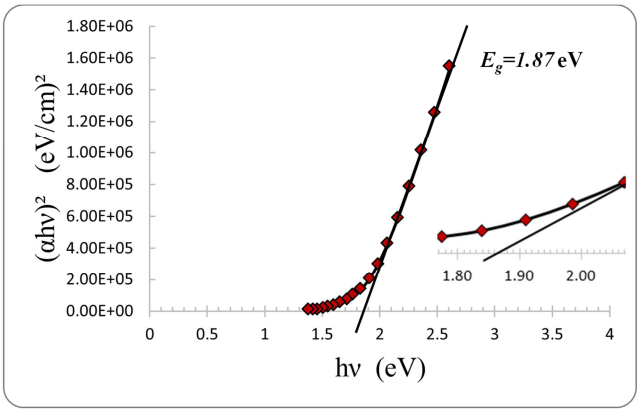

Fig. 6. *$(\alpha h\nu)^2$ values as a function to hν for thin film $LiNi_{0.4}Mn_{1.6}O_4$.*

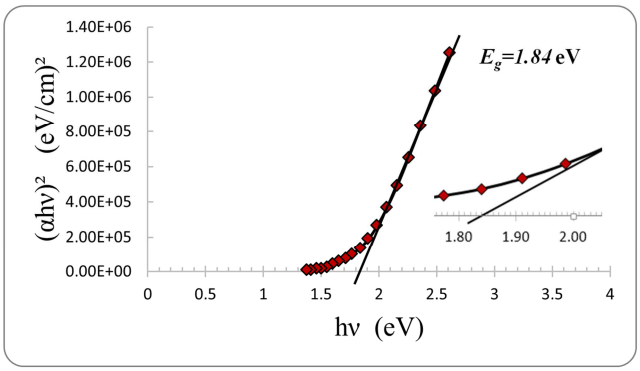

Fig. 7. *$(\alpha h\nu)^2$ values as a function to hν for thin film $LiNi_{0.5}Mn_{1.5}O_4$.*

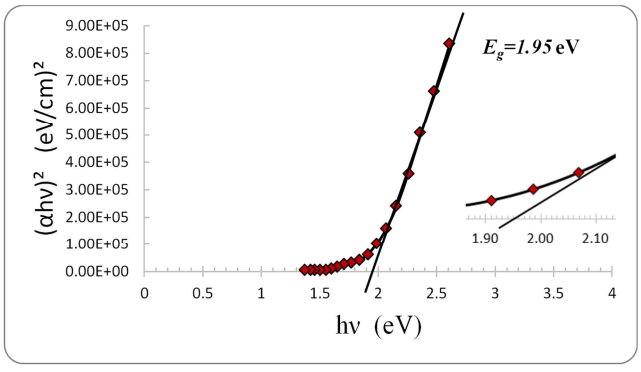

Fig. 8. *$(\alpha h\nu)^2$ values as a function to hν for thin film $LiNi_{0.6}Mn_{1.4}O_4$.*

Table 3. *The values of energy band gab of thin films $LiNi_xMn_{2-x}O_4$.*

Sample	$LiMn_2O_4$	$LiNi_{0.4}Mn_{1.6}O_4$	$LiNi_{0.5}Mn_{1.5}O_4$	$LiNi_{0.6}Mn_{1.4}O_4$
E_g (eV)	2.11	1.87	1.84	1.95

These values are compatible with previous studies where E_g for thin film $LiMn_2O_4$ is 2.25 eV in reference [21]. To indicate the impact of the substitutions ratio x on the energy band gap we draw variation of the energy band gap as a function of Ni content x in spinel $LiNi_xMn_{2-x}O_4$ as shown in Fig. 9.

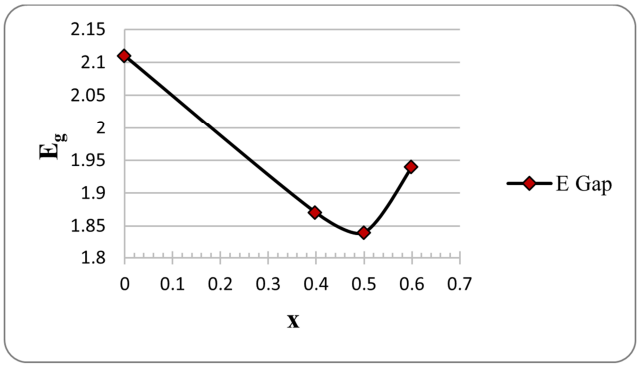

Fig. 9. *Variation of the energy band gap as a function of Ni content x in spinel $LiNi_xMn_{2-x}O_4$.*

As it shown in Fig. 9 the band gap is reduced to a value 1.84 eV for x=0.5. It is well known that the band structure of $LiMn_2O_4$ or Ni-substitute $LiMn_2O_4$ is strongly influenced by hybridization among transition metal 3d and O 2p orbitals, while Li remains in an ionic form. Thus, the decrease in band gap may be explained in terms of the total theoretical density of states (DOS) of pristine $LiMn_2O_4$ and $LiNi_{0.4}Mn_{1.6}O_4$, $LiNi_{0.5}Mn_{1.5}O_4$ thin films [22, 23]. For thin film $LiNi_{0.6}Mn_{1.4}O_4$ there are a slight increase in energy band gap, it may be due to some impurity phases in the structure of this film.

4. Conclusions

In this work, we have prepared thin films $LiNi_xMn_{2-x}O_4$ (x=0, 0.4, 0.5, 0.6) by Sol-Gel method employing spin-coating technique. The films annealed at 600°C for 2 hours. The structural properties of the films were studied by XRD technique. The films were found in cubic spinel structure with decreasing in the lattice constant by increasing the substitution ratio until x=0.5. The decrease of the lattice parameters with Ni substitution in $LiNi_xMn_{2-x}O_4$ can be explained depending on bond length between Mn(Ni) and O in the compound $LiNi_xMn_{2-x}O_4$, this bond increased slightly with Ni substitution because of the larger atomic weight of Ni than Mn, and hence improving structural stability. For x=0.6 a phase transition occur and the structure for this ratio is no longer cubic spinel. The UV-VIS spectra shows that the films have high absorbance in some parts of the visible region, which decreases gradually as the wavelength increases. The direct band gap is reduced from 2.11 eV for $LiMn_2O_4$ to a value 1.84 eV for $LiNi_{0.5}Mn_{1.5}O_4$. The decrease

in band gap may be explained in terms of the total theoretical density of states (DOS) of pristine $LiMn_2O_4$ and $LiNi_{0.4}Mn_{1.6}O_4$, $LiNi_{0.5}Mn_{1.5}O_4$ thin films. For thin film $LiNi_{0.6}Mn_{1.4}O_4$ there are a slight increase in energy band gap, it may be due to some impurity phases in the structure of this film.

References

[1] NOTTEN, P؛ ROOZEBOO, F؛ NIESSEN, R؛ BAGGETTO, L. *3D Integrated All-Solid-State Rechargeable Batteries.* Adv. Mater UK, V. 19, Issue. 24, 2007, 4564–4567.

[2] ARMAND, M؛ TARASCON, M. *Building better batteries.* Nature USA, V. 451, Issue. 7, 2008, 652-657.

[3] DANIEL C. *Materials and processing for lithium-ion batteries*, *Journal of Minerals* Vol. 60, Issu. 9, 2008, 43–48.

[4] GREINER J. MSc Thesis, Massachusetts Institute of Technology, 2006, *Microfabricated thin film batteries Technology and Potential Applications.* 65 pages.

[5] Guyomard, D؛ Tarascon, M; *Li metal-free rechargeable $LiMn_2O_4$ carbon cells: their understanding and optimization*. J. Electrochem. Soc USA, Vol. 139, Issu. 4, 1992, 937-948.

[6] NAKAGAWA, A; KUWATA, N; MATSUDA, Y; KAWAMURA, J, Y. *Thin Film Lithium Battery using Stable Solid Electrolyte Li4SiO4 Fabricated by PLD.* ECS Transactions USA, V. 25, Issue. 36, 2010, 155-161.

[7] WAKIHARA M. *Electrochemical properties of $LiM_{1/6}Mn_{11/6}O_4$ (M = Mn, Co, Al and Ni) as cathode materials for Li-ion batteries prepared by ultrasonic spray pyrolysis method.* Journal of Power Sources USA, Vol. 109, Issue. 2, 2002, 333-339.

[8] NIMISHA, C; YELLARESWAR, K; VENKATESH, G; RAO, G; MUNICHANDRAIA, H. *Sputter deposited LiPON thin films from powder target as electrolyte for thin film battery applications.* Elsevier B. V India, V. 519, Issue. 10, 2011, 3401-3406.

[9] PAULEAU, Y. *Chemical Physics of Thin Film Deposition Processes for Micro- and Nano-Technologies.* 1st, Springer-Science+Business Media, B. V, Lithuania, 2001, 371.

[10] JEFFREY, W. *Recent developments in cathode materials for lithium ion batteries*. Journal of Power Sources USA, Vol. 195, Issu. 4, 2010, 939–954.

[11] KIM, K. *Evolution of the Structural and the Optical Properties and the Related Electronic Structure of $LiT_xMn_{2-x}O_4$ (T = Fe and Ni) Thin Films*. Journal of the Korean Physical Society South Korea, Vol. 51, Issu. 3, 2007, 1166-1171.

[12] NAZARI, G. *Lithium batteries science and technology*. 1st, Springer, USA, 716 pages

[13] XIFEI, L. *Suppression of Jahn–Teller distortion of spinel $LiMn_2O_4$ cathode*, Journal of Alloys and Compounds USA, Vol. 479, Issu. 1-2, 2009, 310–313.

[14] XIAO, X. *Structural and magnetic properties of $LiNi_{0.5}Mn_{1.5}O_4$ and $LiNi_{0.5}Mn_{1.5}O_{4-\delta}$ spinels: A first-principles study*. Chinese Physics *B* China, Vol. 21, Issu. 12, 2012, 128202.

[15] SEYEDAHMADIAN M. *Synthesis and Characterization of Nano sized of Spinel $LiMn_2O_4$ via Sol-gel and Freeze Drying Methods*. Korean Chemical Society, Vol. 34, Issue. 2, 2013, 622-628.

[16] KITTLE C., 2005- Introduction to Solid State Physics. 8th, John Willey & Sons, Inc, USA, 703 pages

[17] DOKKI K. *In situ Raman spectroscopic studies of $LiNixMn_{2-x}O_4$ thin film cathode materials for lithium ion secondary batteries.* Journal of Materials Chemistry, Vol. 12, Issue. 12, 2002, 3688–3693.

[18] KIM K. *Evolution of the Structural and the Optical Properties and the Related Electronic Structure of $LiT_xMn_{2-x}O_4$ (T = Fe and Ni) Thin Films*. Journal of the Korean Physical Society, Vol. 51, Issue. 3, 2007, 1166-1171.

[19] Takahashi K. *Electrochemical and Structural Properties of a 4.7 V-Class $LiNi_{0.5}Mn_{1.5}O_4$ Positive Electrode Material.* Journal of The Electrochemical Society, Vol. 1, Issue. 151, 2004, 173-177.

[20] WIE Y. *Spectroscopic studies of the structural properties of Ni substituted spinel $LiMn_2O_4$. Solid State Ionics*, Vol. 177, Issue. 26-32, 2006, 2201-2838.

[21] Kabir O. *Some Properties of Manganese Oxide (Mn-O) and Lithium Manganese Oxide (Li-Mn-O) Thin Films Prepared via Metal Organic Chemical Vapor Deposition (MOCVD) Technique.* Journal of Materials Science and Engineering B, Vol. 5, Issu. 5-6, 2015, 231-242.

[22] Y. Liu, T. Fuziwara, M. Morinaga, *Electronic structures of lithium manganese oxides for rechargeable lithium battery electrodes.* Solid State Ionics Vol. 126, Issue. 3-4, 1999, 209–218.

[23] S. Shi, C. Ouyang, D.-S. Wang, L. Chen, X. Huang, *The effect of cation doping on spinel $LiMn_2O_4$: a first-principles investigation*. Solid State Commun. Vol. 126, Issue 9, 2003 531–534.